

Field-Induced Magnetic Order and Simultaneous Lattice Deformation in TlCuCl_3

O. Vyaselev,^{1,2} M. Takigawa,^{1,*} A. Vasiliev,³ A. Oosawa,⁴ and H. Tanaka⁵

¹*Institute for Solid State Physics, University of Tokyo, Kashiwanoha, Kashiwa, Chiba 277-8581, Japan*

²*Institute of Solid State Physics, Russian Academy of Science, Chernogolovka, Moscow District 142432, Russia*

³*Department of Low-Temperature Physics, Moscow State University, Moscow 119899, Russia*

⁴*Advanced Science Research Center, Japan Atomic Energy Research Institute, Tokai, Ibaraki 319-1195, Japan*

⁵*Department of Physics, Tokyo Institute of Technology, Oh-okayama, Meguro-ku, Tokyo 152-8551, Japan*

(Received 2 July 2003; published 19 May 2004)

We report the results of Cu and Cl nuclear magnetic resonance experiments and thermal expansion measurements in magnetic fields in the coupled dimer spin system TlCuCl_3 . We found that the field-induced antiferromagnetic transition as confirmed by the splitting of NMR lines is slightly discontinuous. The abrupt change of the electric field gradient at the Cl sites, as well as the sizable change of the lattice constants, across the phase boundary indicate that the magnetic order is accompanied by simultaneous lattice deformation.

DOI: 10.1103/PhysRevLett.92.207202

PACS numbers: 75.30.Kz, 75.80.+q, 76.60.Jx

Quantum phase transitions in spin systems induced by a magnetic field have attracted considerable recent interest [1–8]. An important class of materials is formed by antiferromagnets with a collective singlet ground state at a zero field separated by an energy gap Δ from the first excited triplet. A magnetic field H reduces the gap as $\Delta(H) = \Delta - g\mu_B H$. At $T = 0$, a finite magnetization appears above the critical field $H_c = \Delta/g\mu_B$. Since antiferromagnetic interactions acting among the field-induced spin moments will tilt the magnetization into two sublattices, a Néel order perpendicular to the external field is expected above H_c . This process can be described as the Bose-Einstein condensation of triplet magnons [6,7], since the creation operator of the lowest energy magnon is equivalent to the transverse component of the staggered magnetization. With further increasing the field, some materials show magnetization plateaus at fractional values of the fully saturated moment [3,4], indicating localization of triplets and formation of a superstructure. A wider variety of exotic phases may be expected in the presence of spin-phonon coupling or orbital degeneracy. It is important that these phase transitions can be controlled precisely by tuning the field value, which sets the chemical potential for triplets. Thus spin systems in a magnetic field provide valuable opportunities to test theories on strongly correlated quantum systems.

TlCuCl_3 is a system of three-dimensionally (3D) coupled dimers formed by $S = 1/2$ spins of Cu^{2+} ions with a singlet ground state [5,8]. Although the crystal structure (monoclinic $P2_1/c$ space group) contains Cu_2Cl_6 zigzag chains extending along the a axis as a subunit (Fig. 1) [9], inelastic neutron scattering experiments revealed fully three-dimensional dispersions of triplet magnons [10,11], from which the exchange interactions have been determined. The minimum excitation energy $\Delta \approx 0.5$ meV occurs at $Q = (0, 0, 1)$. The static transverse magnetic order has been observed at the same

Q above a temperature-dependent critical field $H_c(T)$ with $(g/2)H_c(0) = 5.7$ T [12]. Since the dispersion width (7 meV) is much larger than the excitation gap at zero field, the density of triplets is small when the field is close to H_c and the system can be considered as an interacting dilute Bose gas. In fact, mean field [7] and random-phase approximation analysis [13] of a boson model were applied successfully to explain the peculiar shape of the magnetization curve, as well as the excitation spectrum as a function of magnetic field [14–16] in a semiquantitative manner.

In this Letter we report the results of Cu and Cl nuclear magnetic resonance (NMR) experiments and thermal expansion measurements on TlCuCl_3 near the critical field. The antiferromagnetic order was confirmed by the splitting of NMR lines. The staggered magnetization develops discontinuously and the paramagnetic and antiferromagnetic phases coexist in a narrow region in the H - T plane, pointing to a weakly first-order phase transition. We found also that the electric field gradient at the Cl sites changes abruptly across the phase boundary, indicating that a lattice deformation occurs simultaneously at the magnetic transition. This is further confirmed by a sizable change of the lattice parameter

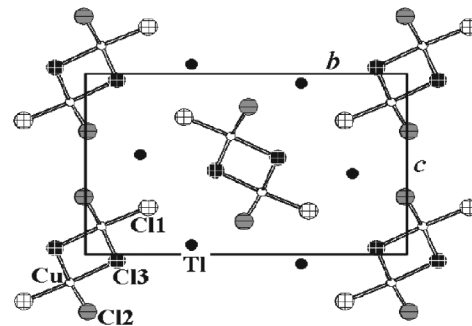


FIG. 1. The crystal structure of TlCuCl_3 viewed along the a axis.

measured by the strain gauge technique in the magnetic field.

As shown in Fig. 1, a monoclinic unit cell of TiCuCl_3 contains 4 f.u. When the magnetic field is along or perpendicular to the b axis, the four units give identical NMR lines. All the measurements were performed in the external field perpendicular both to the b axis and approximately to the $(10\bar{2})$ plane. Thus one Cu and three Cl sites should be distinguished. There are six Cu NMR lines in the absence of magnetic order: each of the two spin-3/2 isotopes, ^{63}Cu and ^{65}Cu , generates three lines split by electric quadrupole interaction. The Cu NMR data were taken on the central transition ($-1/2 \leftrightarrow 1/2$) line from ^{63}Cu . For Cl NMR, we found that 18 lines (three quadrupole split lines for each of two spin-3/2 isotopes, ^{35}Cl and ^{37}Cl , from three sites) are congested in a relatively narrow frequency range. Fortunately, a pair of outermost lines corresponding to the low-frequency quadrupole satellite of ^{37}Cl and high-frequency satellite of ^{35}Cl from the same Cl site are isolated from other lines. We used these lines to obtain Cl NMR data, although we have been unable to assign the specific sites to which these lines correspond. The thermal expansion was measured by the strain gauge technique. The strain gauge was calibrated using the spontaneous strain along the a axis at the phase transition in α' - NaV_2O_5 [17]. The gauge was attached to the $(10\bar{2})$ plane along the b axis. To correct for the magnetoresistance of the gauge, the curves taken in different fields have been shifted to merge at high temperatures.

Figure 2 shows the frequency shifts for the central transition of ^{63}Cu (a) and for the pair of Cl satellites (b) as a function of temperature at $H = 8.56$ T. The shifts are defined as ${}^n\Delta\nu = {}^n\nu - {}^n\gamma H$, where ${}^n\nu$ is the peak frequency of the n th nuclei with the gyromagnetic ratio ${}^n\gamma$. The main feature is the splitting of all lines into two branches ${}^n\Delta\nu^\pm$ below 5.6 K, which coincides the Néel temperature (T_N) for $H \parallel [10\bar{2}]$ at 8.56 T [8].

Generally, the shift of ^{63}Cu NMR is the sum of the magnetic and quadrupolar parts. For the central transition, the quadrupolar part contains only the second and higher order terms ${}^{63}\Delta\nu_Q^{(2)}$. The magnetic part is due only to the uniform magnetization ${}^{63}\Delta\nu_u$ above T_N , but the contribution from the staggered magnetization ${}^{63}\Delta\nu_s$ adds below T_N . Thus ${}^{63}\Delta\nu = {}^{63}\Delta\nu_u + {}^{63}\Delta\nu_Q^{(2)}$ above T_N and ${}^{63}\Delta\nu^\pm = {}^{63}\Delta\nu_u + {}^{63}\Delta\nu_Q^{(2)} \pm {}^{63}\Delta\nu_s$ below T_N . It should be noted that even though the staggered magnetization is perpendicular to the external field, anisotropic hyperfine interactions generally produce a finite component of staggered local field at the nuclei, ${}^n h_s = {}^n \Delta\nu_s / {}^n \gamma$, parallel to the external field. The staggered contribution below T_N cancels for the mean value ${}^{63}\Delta\nu \equiv ({}^{63}\Delta\nu^+ + {}^{63}\Delta\nu^-) / 2 = {}^{63}\Delta\nu_u + {}^{63}\Delta\nu_Q^{(2)}$.

We plot ${}^{63}\Delta\nu$ (for $T \geq T_N$), ${}^{63}\Delta\nu$ (for $T \leq T_N$), and ${}^{63}h_s$ against temperature in Figs. 3(a) and 3(b). Since the temperature variation of ${}^{63}\Delta\nu_Q^{(2)}$ below 7 K is expected

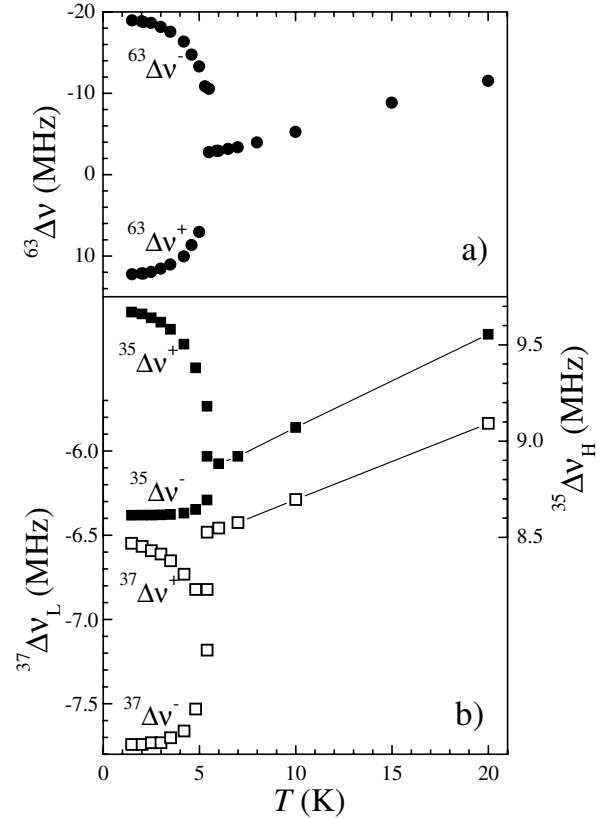


FIG. 2. Temperature dependencies of NMR frequency shifts at $H = 8.56$ T. (a) Central transition of ^{63}Cu . (b) High-frequency satellite of ^{65}Cl (closed squares, right axis) and low-frequency satellite of ^{37}Cl (open squares, left axis).

to be negligibly small, the change of ${}^{63}\Delta\nu$ and ${}^{63}\Delta\nu$ should be due to the temperature variation of the uniform magnetic shift, ${}^{63}\Delta\nu_u$. Indeed, the plot in Fig. 3(a) is quite similar to the temperature dependence of the bulk magnetization [5], including the characteristic cusplike minimum at T_N .

The staggered local field ${}^{63}h_s$ rises very sharply at T_N . The spectrum at 5.5 K consists of a single line originating from the paramagnetic phase and a pair of split lines coming from the antiferromagnetic phase. With increasing temperature, the intensity of the latter vanishes within about 0.2 K. The same feature was seen in the evolution of the Cl NMR spectra as shown in Fig. 3(c). At 5.6 K, one can clearly see the coexistence of a single peak and a pair of split peaks. Moreover, tracking the temperature evolution from 5.2 K upwards, one notices that the split lines do not merge to become a single line. Instead, the intensity of the split lines vanishes between 5.7 and 5.8 K, while the interval of the splitting is still finite. We observed no hysteresis for up and down temperature sweep. The coexistence of two phases is clearly due to some kind of disorder. The appearance of the split spectrum, however, indicates that the staggered magnetization develops discontinuously upon entering into the antiferromagnetic phase. Thus the transition is weakly

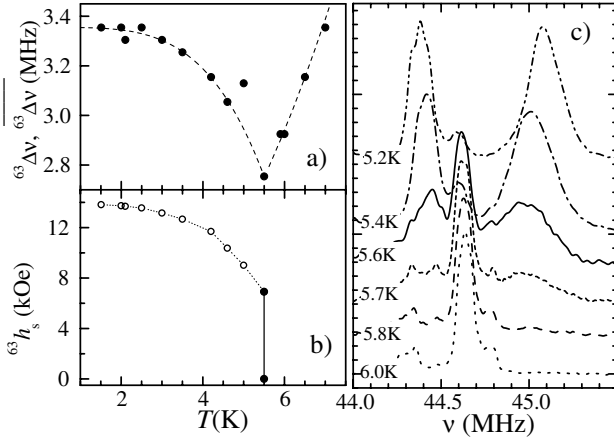


FIG. 3. (a) Uniform frequency shift for the ^{63}Cu central transition. The line is a guide to the eye. (b) The staggered hyperfine field obtained from the splitting of the ^{63}Cu central line. At 5.5 K, the spectrum consists of unsplit ($^{63}h_s = 0$) and split (finite $^{63}h_s$) lines. (c) Evolution of the high-frequency satellite ^{35}Cl NMR spectrum across the phase boundary. All data were taken at $H = 8.56$ T.

first order. We also observed the same feature at a fixed temperature $T = 3.5$ K with increasing magnetic field across the phase boundary near 6.3 T.

We emphasize that the discontinuity of the transition observed by NMR is not in contradiction with the continuous development of the antiferromagnetic Bragg peaks observed by neutron diffraction experiments [12]. The intensity of the Bragg peaks represents the square of the staggered moment averaged over the entire sample volume. If the volume fraction of the antiferromagnetic phase changes continuously over a finite temperature window near T_N as evidenced by the evolution of the Cl NMR spectrum, a locally discontinuous transition should look like a continuous one when averaged over the entire volume.

Another important feature of the field-induced transition was revealed by the behavior of the quadrupole splitting of the Cl NMR spectrum. Above T_N , the shifts for the high-frequency ^{35}Cl satellite and low-frequency ^{37}Cl satellites plotted in Fig. 2(b) are expressed by

$$\begin{aligned} {}^{35}\Delta\nu_H &= {}^{35}\Delta\nu_u + {}^{35}\Delta\nu_Q^{(2)} + {}^{35}\Delta\nu_Q^{(1)}, \\ {}^{37}\Delta\nu_L &= {}^{37}\Delta\nu_u + {}^{37}\Delta\nu_Q^{(2)} - {}^{37}\Delta\nu_Q^{(1)}, \end{aligned} \quad (1)$$

where $\Delta\nu_Q^{(1)}$ is the first-order quadrupole shift. This is determined by the magnitude of the electric field gradient along the external field direction. The temperature dependence of $\Delta\nu_Q^{(1)}$ reflects the change of lattice parameters and ionic charge distribution within a unit cell. Below T_N , the staggered shift adds to Eqs. (1): ${}^{35}\Delta\nu_H^\pm = {}^{35}\Delta\nu_H \pm {}^{35}\Delta\nu_s$, ${}^{37}\Delta\nu_L^\pm = {}^{37}\Delta\nu_L \pm {}^{37}\Delta\nu_s$. Note that $\Delta\nu_s$ cancels for the mean values, $\overline{{}^n\Delta\nu_{H(L)}} \equiv (\overline{{}^n\Delta\nu_{H(L)}^+} + \overline{{}^n\Delta\nu_{H(L)}^-})/2$, so below T_N , $\overline{{}^n\Delta\nu_{H(L)}}$ replaces the left-hand side of Eqs. (1). Using the isotopic ratio of each term in

Eqs. (1)

$$\begin{aligned} {}^{37}\Delta\nu_u/{}^{35}\Delta\nu_u &= {}^{37}\gamma/{}^{35}\gamma \equiv r_\gamma \approx 0.83, \\ {}^{37}\Delta\nu_Q^{(1)}/{}^{35}\Delta\nu_Q^{(1)} &= {}^{37}Q/{}^{35}Q \equiv r_Q \approx 0.79, \\ {}^{37}\Delta\nu_Q^{(2)}/{}^{35}\Delta\nu_Q^{(2)} &= r_Q^2/r_\gamma \approx 0.87, \end{aligned} \quad (2)$$

where nQ is the quadrupole moment of the n th nucleus, one obtains ${}^{35}\Delta\nu_Q^{(1)}$ as

$$\begin{aligned} (r_\gamma {}^{35}\Delta\nu_H - {}^{37}\Delta\nu_L)/(r_\gamma + r_Q) &= \\ {}^{35}\Delta\nu_Q^{(1)} + {}^{35}\Delta\nu_Q^{(2)}(r_\gamma - r_Q)/r_\gamma &\approx {}^{35}\Delta\nu_Q^{(1)} \end{aligned} \quad (3)$$

for $T > T_N$. For $T < T_N$, ${}^n\Delta\nu_{H(L)}$ should be replaced by $\overline{{}^n\Delta\nu_{H(L)}}$. Since ${}^{35}\Delta\nu_Q^{(2)} \ll {}^{35}\Delta\nu_Q^{(1)}$ and $(r_\gamma - r_Q)/r_\gamma = 0.05$, the second term on the right-hand side can be safely neglected.

The temperature dependence of ${}^{35}\Delta\nu_Q^{(1)}$ is plotted in Fig. 4(a). There is a clear jump in ${}^{35}\Delta\nu_Q^{(1)}$ at T_N , indicating a sudden change in the atomic positions and/or lattice parameters. The change of lattice parameters was directly detected by the thermal expansion measurements. In Fig. 4(b), the relative change of the crystal size along the b axis, $\Delta b/b$, is plotted against temperature for different magnetic fields. Anomalous expansion is observed below a field-dependent onset temperature, which coincides with T_N . The magnitude of the strain is linear in field as shown in the inset in Fig. 4(b). Measurement of the strain along the a axis has shown that $\Delta a/a$ is negative and an order of magnitude smaller than $\Delta b/b$. The c -axis strain could not be measured properly. The change of the lattice parameters, however, is very small and this alone would not be sufficient to account for the

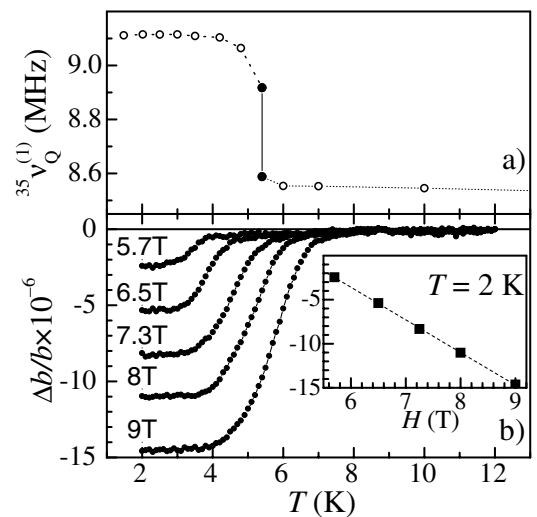


FIG. 4. (a) First-order quadrupole shift for ^{35}Cl extracted with Eq. (3) from the data in Fig. 2(b). (b) b -axis thermal expansion in different magnetic fields. The inset shows the b -axis strain vs magnetic field at 2 K.

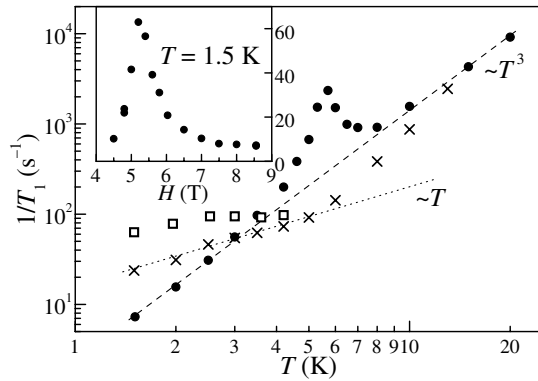


FIG. 5. Temperature dependence of ^{63}Cu spin-lattice relaxation rate at $H = 5.2$ T (squares), 4.8 T (crosses), and 8.5 T (circles). Inset: field dependence of the relaxation rate at 1.5 K.

large change of $^{35}\Delta\nu_Q^{(1)}$. There must be sizable displacement of the ionic positions within a unit cell.

The results presented so far convincingly demonstrate that lattice deformation occurs simultaneously with the magnetic phase transition. Thus the Bose-Einstein condensation scenario within a pure spin model is not adequate and spin-phonon coupling has to be taken into account for a quantitative description of the field-induced phase transition. Strong spin-phonon coupling has also been suggested by the recent observation of pressure-induced antiferromagnetic order [18]. It is known in classical magnets that strong enough magnetoelastic coupling turns an otherwise second order magnetic transition into a first-order one accompanying magnetostriction [19]. It is likely that a similar mechanism works in the present case of a quantum phase transition. However, it is still possible that specific interactions among bosons in this material are the driving force for the first-order transition.

The fact that the transition is only marginally discontinuous is also indicated by a quasicritical slowing down of the spin fluctuations observed by the nuclear spin-lattice relaxation rate measurements. The spin-lattice relaxation rate, $1/T_1$, of ^{63}Cu nuclei is plotted against temperature in Fig. 5 for the external fields of 4.8, 5.2 (the zero-temperature critical field), and 8.5 T. The inset shows the field dependence of $1/T_1$ at 1.5 K. The data at 8.5 T clearly show a sharp peak at T_N . Above 8 K, $1/T_1$ increases approximately as T^3 . Such a temperature dependence indicates that the major weight of the spin fluctuations has an energy scale much larger than T_N . At lower temperatures, the relaxation rate at 4.8 T switches to linear T dependence, and $1/T_1$ at 5.2 T is nearly independent of temperature. The relaxation rate at the phase boundary is sharply peaked, as seen in the T dependence at $H = 8.5$ T and in the H dependence at

$T = 1.5$ K. Such behavior of $1/T_1$ is due to a slowing down of the fluctuations of staggered moments in the vicinity of the phase boundary, which is common for continuous antiferromagnetic transitions.

In conclusion, we clarified some new features of the field-induced magnetic order in TlCuCl_3 . Splitting of the NMR peaks in the field-induced phase reveals a long range Néel order. The staggered local field is shown to arise discontinuously, indicating that the transition is weakly first order. Sizable deformation of the lattice due to the magnetic ordering is detected in both NMR and thermal expansion measurements, which implies strong spin-phonon coupling and possibly explains the first-order nature of the transition. The spin-lattice relaxation rate is sharply peaked at the phase boundary due to a quasicritical slowing down of the fluctuations of staggered magnetization.

The authors acknowledge fruitful discussions with K. Ueda and M. Zhitomirsky. The work is supported by the Grant-in-Aid for Scientific Research on Priority Area (B) on “Field-induced new quantum phenomena in magnetic systems” from Ministry of Education, Culture, Sports, Science, and Technology of Japan. The research activity of O.V. in Japan was supported by the Japan Society for Promotion of Science.

*Electronic address: masashi@issp.u-tokyo.ac.jp

- [1] T. M. Rice, *Science* **298**, 760 (2002).
- [2] G. Chaboussant *et al.*, *Eur. Phys. J. B* **6**, 167 (1998).
- [3] K. Kodama *et al.*, *Science* **298**, 395 (2002).
- [4] W. Shiramura *et al.*, *J. Phys. Soc. Jpn.* **67**, 1548 (1998).
- [5] A. Oosawa, M. Ishii, and H. Tanaka, *J. Phys. Condens. Matter* **11**, 265 (1999).
- [6] T. Giamarchi and A. M. Tsvelik, *Phys. Rev. B* **59**, 11 398 (1999).
- [7] T. Nikuni, M. Oshikawa, A. Oosawa, and H. Tanaka, *Phys. Rev. Lett.* **84**, 5868 (2000).
- [8] A. Oosawa, H. Aruga Katori, and H. Tanaka, *Phys. Rev. B* **63**, 134416 (2001).
- [9] R. D. Willett, C. Duggins, Jr., R. F. Kruh, and R. E. Rundle, *J. Chem. Phys.* **38**, 2429 (1963).
- [10] A. Oosawa *et al.*, *Phys. Rev. B* **65**, 094426 (2002).
- [11] N. Cavadini *et al.*, *Phys. Rev. B* **63**, 172414 (2001).
- [12] H. Tanaka *et al.*, *J. Phys. Soc. Jpn.* **70**, 939 (2001).
- [13] M. Matsumoto, B. Normand, T. M. Rice, and M. Sigrist, *Phys. Rev. Lett.* **89**, 077203 (2002).
- [14] N. Cavadini *et al.*, *Phys. Rev. B* **65**, 132415 (2002).
- [15] Ch. Rüegg *et al.*, *Appl. Phys. A (Suppl.)* **74**, S840 (2003).
- [16] Ch. Rüegg *et al.*, *Nature (London)* **423**, 62 (2003).
- [17] M. Köppen *et al.*, *Phys. Rev. B* **57**, 8466 (1998).
- [18] A. Oosawa *et al.*, *J. Phys. Soc. Jpn.* **72**, 1026 (2003).
- [19] T. Ito, K. Ito, and M. Oda, *Jpn. J. Appl. Phys.* **17**, 371 (1978).